New Methods of Nuclear Quadrupole Resonance *

V. S. Grechishkin

Kaliningrad State University, 14, A. Nevsky Street, 23041 Kaliningrad, USSR

Z. Naturforsch. **45a**, 559–564 (1990); received August 23, 1989

New NQR methods, developed over the past years, are discussed: 1. Two frequency NQR double resonance, 2. the influence of strong off-resonance combination of rf pulses on demagnetized state in NQR, 3. remote NQR.

Direct NQR signals from the light nuclei ^2H, ^{10}B, ^{14}N use to be weak; their detection is difficult. For these light nuclei nuclear quadrupole double resonance (DNQR) methods are preferable in which the sensitivity is enhanced due to the thermal contact of two spin-systems and indirect detection. The higher the initial magnetic field B_0, the better is the DNQR sensitivity. Apart from this, the DNQR sensitivity is dependent on the efficiency and duration of thermal contact between the quadrupole and magnetic systems.

We have shown [1] that, if the sample in the applied zero magnetic field is saturated simultaneously by two NQR frequencies, the proton magnetization is destroyed much more effectively. The two-frequency saturation of a quadrupole system leads to increased DNQR sensitivity, thus allowing the assignment of lines to the equivalent nuclei in multiple spectra [2]. For the ν_--line in $^{14}N-^{1}H$ DNQR spectra which have the lowest intensity, the two-frequency saturation considerably increases the intensity.

If the sample in the applied zero magnetic field is irradiated by the rf field $\omega_P \pm \omega_Q$, the thermal contact is realized due to the solid effect. ω_Q is the NQR frequency and ω_P is the proton NMR frequency in the local magnetic field. It follows from the solid effect analysis [3], that the most intensive line is the $\omega_Q + \omega_P$ one. In some cases two frequency irradiation also increases the solid effect satellite intensities.

The efficiency of thermal contact between the proton and quadrupole systems may be increased by the selective magnetic field technique, see Figure 1 and [4, 5], provided both, the proton spin-lattice relaxation time T_{1D} in the applied zero magnetic field and the quadrupole relaxation time T_{1Q} are sufficiently long. After saturation of the quadrupole system the sample is transported to the intermediate magnetic field H_S and level crossing $\gamma H_S = \omega_Q$ takes place. On spectrum recording frequency ω_Q is swept slowly and simultaneously transformed into a voltage which changes synchronously with ω_Q and the magnetic field B_S provided by a special solenoid.

There is another effective technique of NQR investigations [1]. The joint use of adiabatic demagnetization in NQR and Fourier-transform technique reduces the time of the experiment and allows the detection of unbroadened lines. The experimental cycles of DNQR on the other hand are very long. The first experimental results by NQR with adiabatic demagnetization were reported in [6]. The thermal contact through level crossing with a proton system previously cooled by adiabatic demagnetization reduces the quadrupole spin temperature and subsequently decreases the NQR signal intensity, see Figure 2. To obtain the best thermal contact, multi-level-crossing is most effective. In the applied zero magnetic field the proton magne-

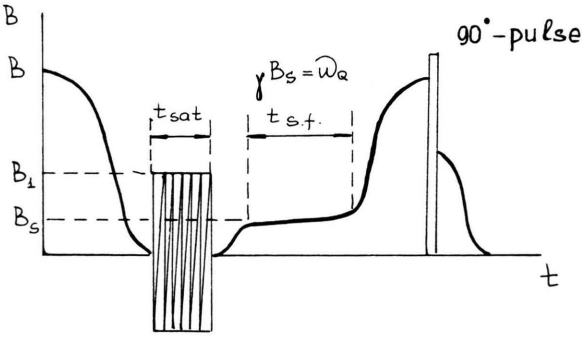

Fig. 1. Time diagram of DNQR with a selective field.

---

* Presented at the Xth International Symposium on Nuclear Quadrupole Resonance Spectroscopy, Takayama, Japan, August 22–26, 1989.

Reprint requests to Prof. V. S. Grechishkin, Kaliningrad State University, 14, A. Nevsky Street, 23041 Kaliningrad, USSR.

0932-0784 / 90 / 0300-0559 $ 01.30/0. – Please order a reprint rather than making your own copy

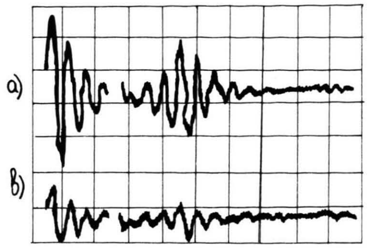

Fig. 2. ^{14}N signals in $CO(NH_2)_2$ for $\nu_+ = 2.913$ MHz: a) after sample adiabatic demagnetization, b) in the absence of sample adiabatic demagnetization; the horizontal scale is 1 ms, $T = 77$ K, $\nu_P = 17.0$ MHz.

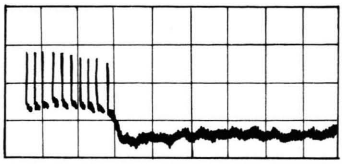

Fig. 3. Ten-pulse spin-locking at 77 K for ν_+ in urea after adiabatic demagnetization.

tization is given by

$$M(t) = M_0 \exp(-t/T_{1D}),$$

where the proton relaxation time T_{1D} in zero magnetic field is less than the proton spin-lattice relaxation time T_1 ($T_{1D} \ll T_1$) for solids. Since T_{1D} is small compared to the sample transfer time, multilevel-crossing in many cases is not obtainable.

As reported in [7], the sequence of strong rf pulses is used in order to achieve a multiple contact of magnetic and quadrupole systems. When the pulse width in the sequence is about 30 µs and time intervals (τ) between pulses comparable with the spin-spin relaxation time T_2 ($\tau \approx T_2$), spin-locking is feasible [8] without preparation pulse. For urea at $T = 77$ K the ^{14}N quadrupole system induction decay with a time constant T_{1P} in the rotating frame lasts for about one minute (Figure 3). It allows numerous induction signals appearing in the pulse intervals to be stored during the spin-locking.

The spin systems of nitrogens and protons are in thermal contact in the rotating frame if the Hartmann-Hahn relation [9] is realized

$$\sqrt{2}\,\gamma_N H_1 = \gamma_H H_2, \tag{1}$$

where γ_N and γ_H are the gyromagnetic relations of nitrogen and proton, respectively. H_1 is the field amplitude with the NQR frequency of ^{14}N and H_2 is the local magnetic field in the crystal.

The inverse spin temperatures of protons (β_J) and nitrogens (β_S) during thermal contact can be described by

$$\begin{aligned} \beta_J(t) &= (\beta_{J_0} - \beta_f)\exp(-t/T_{JS}) + \beta_f, \\ \beta_S(t) &= \beta_f\,[1 - \exp(-t/T_{JS})], \end{aligned} \tag{2}$$

where β_f is the final temperature after n contacts and β_{J_0} is the initial spin temperature of the proton system after the sample transfer from the high magnetic field.

The magnetization of the nitrogen spin system after thermal contact is given by

$$M_S = \frac{\gamma_H}{\gamma_N}\,\frac{1}{17a}\,M_{S_0}, \tag{3}$$

where $a = C_S H_1^2 / C_J H_2^2$; C_S and C_J are the Curie-constants for S and J nuclei, respectively.

With an interpulse interval $\tau = 300$ µs and urea, $CO(NH_2)_2$, at 77 K as sample, 1000 contacts have been realized during 0.4 s. This is less than the proton relaxation time T_{1D} in urea (≈ 60 s at 77 K). The induction signal storage in interpulse intervals has increased the ^{14}N NQR signal intensity in urea by 100 times. The technique described yields a substantial gain in DNQR. The method of cycling field, an integral part of DNQR, is also extensively employed in NMR-spectroscopy [10]. It is characterized by high sensitivity and high resolution.

In recent years a number of papers [11–14] reported field cycling experiments in which nuclear quadrupole free precession is developed in zero field and detected either after the first field switching or by applying a train of pulses of applied magnetic field. Fourier-transformation of the sample magnetization, measured at high field as a function of the sample residence time in zero field, gives the pure quadrupole resonance spectrum. The application of a magnetic field in the form of video pulses to initiate the magnetization evolution is not influenced by the rate of magnetic field switching. In the experiments nuclei are selectively excited, thus, e.g., for ^{2}H and ^{14}N there is no proton dipolar absorption obscuring the low frequency lines. It is difficult to make a theoretical analysis of these experimental results, therefore [11, 12] failed to obtain mathematical expressions for the signal intensities in NQR spectra (for J = I) detected by adiabatic cycling field technique.

We have analysed some ^{14}N NQR results obtained by video pulse magnetic field and adiabatic demagnetization techniques. The results of this analysis are

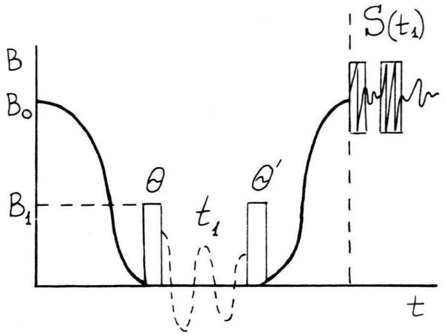

Fig. 4. Time diagram of cycling field [11].

useful for the interpretation of spectra and optimum parameter choice of the applied saturation program. In particular, we consider a case of the program shown in Figure 4. The first d.c. field (Θ) transforms the stationary quadrupole and protons magnetization induced in the process of adiabatic demagnetization and thermal contact through level crossing; it initiates its coherent evolution during the time t_1. After a time period t_f the evolution is terminated by a second d.c. pulse (Θ'). The sample is remagnetized and level crossing takes place in inverse order. The proton magnetization which results in the high magnetic field is modulated by the NQR frequencies of nitrogen atoms connected to protons.

We shall assume that a homonuclear system of nitrogen spins and their signal $S(t)$ is not distorted during indirect detection. Neglecting the hetero- and homonuclear dipolar coupling in the zero magnetic field and assuming a homogeneous distribution of crystallites in the powder we write

$$\begin{aligned} S(t_1) = S_P\,[H_Q \exp(-i\Theta' H_1)\exp(-iH_Q t) \\ \cdot \exp(-i\Theta H_1)\,\varrho(0)\exp(i\Theta H_1) \\ \cdot \exp(iH_Q t_1)\exp(i\Theta' H_1)], \end{aligned}$$

where H_Q is Hamiltonian of quadrupole interactions, H_1 is the Hamiltonian of the interactions with the field B_1, $\varrho(0) = \beta_Q H_Q$ and β_Q is the inverse spin temperature of the quadrupole system.

Integrating over the powder distribution and considering the simple case $\Theta = \Theta'$ we obtain

$$\begin{aligned} \overline{S(t_1)} = A(\alpha) + [B(\alpha)(\omega_+^2 + \omega_-^2) + C(\alpha)\,\omega_0^2] \cos \omega_0 t_1 \\ + [B(\alpha)(\omega_-^2 + \omega_0^2) + C(\alpha)\,\omega_+^2] \cos \omega_+ t_1 \\ + [B(\alpha)(\omega_+^2 + \omega_0^2) + C(\alpha)\,\omega_-^2] \cos \omega_- t_1, \qquad (5) \end{aligned}$$

where $A(\alpha)$ is time independent component

$$\begin{aligned} B(\alpha) = (4\hbar^2/315)(\cos\alpha - 1)^2 \\ \cdot (10\cos^2 + 10\cos\alpha + 1), \qquad (6) \end{aligned}$$

and

$$\begin{aligned} C(\alpha) = (4\hbar^2/105)(\cos\alpha - 1) \\ \cdot (10\cos^3\alpha + 16\cos^2\alpha + 8\cos\alpha + 1). \quad (7) \end{aligned}$$

From (5) it follows that the intensities of the NQR lines ω_0, ω_-, ω_+ differ; they depend on the parameter $\alpha = \gamma H_1 \Theta$. The dependence of (5) on α is identical for different magnitudes of the asymmetry parameter η. Provided $\alpha = \pi$, the NQR lines intensities have the same magnitudes and equal phases. If $\alpha = 0.1\,\pi$, then the phases of lines ω_+ and ω_- are inverted with respect to ω_0. This fact should be considered in the spectra interpretation. Adding the third d.c. pulse and detecting the signal $S(t_1, t_2)$ at times t_1 and t_2 makes it possible to employ two-dimensional spectroscopy technique for spectra analysis.

In [15], for instance, the line assignment in the NQR spectrum is made by cross-peaks of two-dimensional spectroscopy. It is noted that additional echo signals [16] in the two-frequency NQR spectroscopy are equivalent to cross-peaks in the two-dimensional NMR spectroscopy. However, the two-frequency method was proposed much earlier. The time necessary to perform the experiment in the two-dimensional spectroscopy in zero field is very long because for Fourier-transform of two-dimensional function $S(t_1, t_2)$ quite a number of points should be fixed and sometimes, in addition, signal storage is necessary.

In contrast to the rf pulse technique [1], the video pulse technique does not permit synchronous rectification in zero field. Therefore the signals are indirectly detected. The excitation of a ^{14}N NQR system by video pulses in zero field is, to a considerable extent, equivalent to noise excitation; signal storage in zero field is not possible [17]. It should be noted that the technique with cycling field, video pulses of magnetic field irradiation, and indirect detection for ^{2}D, ^{14}N NQR has considerable power in the frequency range below 1 MHz. At higher frequencies the rf technique may be used.

The ability and the specific characteristics of remote NQR are widely discussed in literature. Remote NQR involves cases where the sample is separated by opaque materials from the instrument: Mines, drugs and explosives in packages, quality analysis of solids in process streams, bulk solids analysis, mineral resources prospecting, and others. NQR is known to be a highly specific detector of chemical compounds and of nuclei in chemically non-equivalent positions. It also allows the detection of narrow lines, and unambiguous identification of chemical structures.

One of the most serious disadvantages of the NQR method applied to remote sample search results from its low sensitivity, especially in the low frequency range. At low temperatures it is a problem to detect signals from samples placed within the spectrometer coil. A substantial increase in spectrometer sensitivity required for the local NQR usage can be obtained [1] by:

- a scale-up in the amount of a sample,
- a considerable background decrease (noise, broadcasting signals, etc.) through time selectors, selective bucking coils, etc.,
- efficient use of storage time by means of multipulse sequencies,
- employment of Fourier-transform technique, automation of the measurement, and correlation spectroscopy.

It is noted that the application of the NQR method for the detection of remote objects was demonstrated for the first time in 1972 by Grechishkin and Shishkin [16].

In contrast with NMR spectroscopy, local NQR does not require a magnetic field. On the other hand, because of low NQR signal intensity and the use of solid samples, there is little feasibility in obtaining NQR images. Presently, it is only possible to detect NQR signals from a large bulk of a sample situated outside the spectrometer sensor.

For the local NQR a flat pancake transmitter-receiver coil may be used. It is placed over the sample (Figure 5). The radio frequency field being non-homogeneous, the coil detects signals from the sample volume limited by the coil radius.

The maximum induction signal [1] after the radio frequency pulse impact on a powder sample with the radio frequency field H_1 being uniform, is given by

$$\langle J_i \rangle H_1 = \frac{N \hbar \omega_Q}{3kT} \left(\frac{\sin P - P \cos P}{P^2} \right), \tag{8}$$

where $P = 2\gamma H_1 t_w$ and $i = x, y, z$.

To obtain a 90° rf pulse the following equation should be fulfilled:

$$2\gamma H_1 t_w = 0.66\,\pi\,. \tag{9}$$

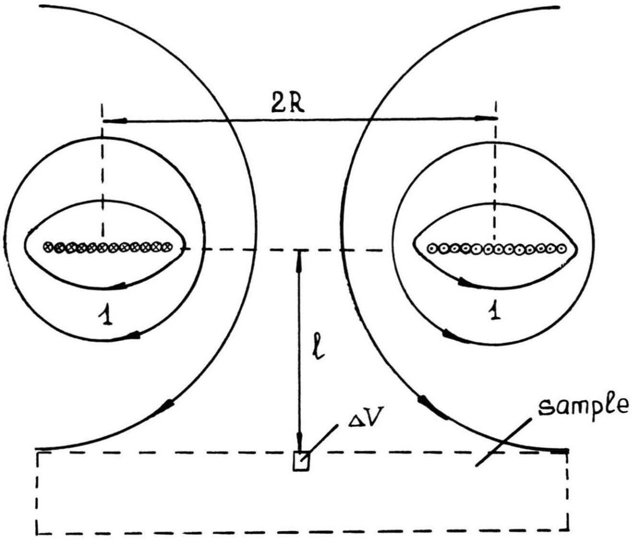

Fig. 5. The field structure around a sample.

For remote NQR experiments a standard pulse NQR spectrometer is designed to operate in the nitrogen frequency range with a ribbon pancake coil and optimized sensor. The pancake coil and sample bulk being large, (9) cannot be fulfilled because of the inhomogeneous field H_1.

At first, as the rf pulse width increases, the amplitude of induction signal also intensifies, and afterwards it remains practically constant.

In our experiments we employed pancake coils of two configurations. The first one is a spiral wound ribbon conductor coil with a 50 mm inner diameter and a 100 mm outer diameter. The second one is a spiral ribbon coil made on printed-circuit card of fibre-glass laminate with a 200 mm diameter. Enlarging the coil diameter enhances the sensitivity but the background increases, too.

For the first coil with the distance between the sample and the coil equal to zero, the rf pulse width is about 40 µs. Crystal powder of $C_6H_{12}N_4$ (hexamethylenetetramine) is placed in a cylindrical container with a diameter equal to the outer coil diameter and height of 10 mm. From (9) the field intensity near the coil is calculated as $H_1 \approx 14$ G.

The dependence of ^{14}N NQR signal in hexamethylenetetramine from the distance between the sample and the coil is shown in Figure 6.

The magnetic moment of the sample volume element ΔV (Fig. 5) located on the coil axis at a distance

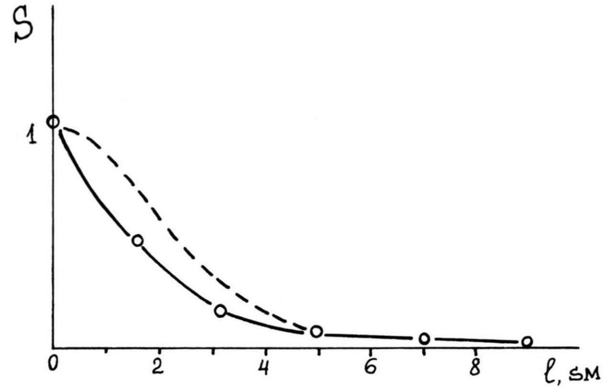

Fig. 6. The dependence of ^{14}N NQR signal in hexamethylenetetramine ($C_6H_{12}N_4$) on the distance between the sample and the ribbon coil ($\Delta\omega = 3$ kHz).

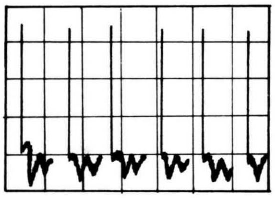

Fig. 7. ^{14}N NQR signal in hexamethylenetetramine ($C_6H_{12}N_4$) at 300 K. Six pulse sequence effect ($\Delta f = 2.3$ kHz, $t_w = 30$ µs; $\tau = 1.4$ µs).

l from the coil is given by

$$M = \gamma \hbar \langle J_i \rangle H_i \,. \tag{10}$$

At this point it is collinear to the induction vector $\boldsymbol{B}_1$

$$B_1 = \frac{\mu \mu_0 J R^2}{2(R^2 + l^2)^{3/2}} \,. \tag{11}$$

For simplicity we assume that there is a single turn conductor with radius R and current J.

Taking (6) into acccount, the e.m.f. induced by V in this coil is determined by

$$\varepsilon = \frac{\mu \mu_0 \gamma \hbar^2 \omega_Q^2 N}{6 k \pi} \frac{R^2}{(R^2 + l^2)^{3/2}} \cdot \left(\frac{\sin P - P \cos P}{P^2} \right) \cos \omega_Q^2 t, \tag{12}$$

where B_1 is defined by (10), (11).

For a 90° pulse, the functional dependence of the induction signal from the distance is shown by the dashed line in Figure 5. In practice, however, the field B_1 is not uniform, and the signal dependence on the distance, volume and sample configuration becomes much more complicated. The coil (Fig. 5) does not appear to be optimum, its most effective area being near the region (1). The most updated design of transmitter and receiver is a system of two parallel fed multiturn coils.

Since (9) cannot be fulfilled while the peak voltage and transmitter power for a given field are maintained at reasonable levels, a special coherent multipulse sequence must be applied.

A 90° pulse sequence with a time width t_w and in the time of order $\tau < T_2$ resonant to pure quadrupole transitions in response evokes a magnetization which persists for a long time.

If there are off-resonance pulses (Δf) then the magnetization M_x is determined by

$$M_x = M_0 \frac{B_0 (2\pi \,\Delta t/\gamma)}{B_1^2 + B_{\text{loc}}^2 + (2\pi \,\Delta t/\gamma)^2} \,, \tag{13}$$

where M_0 is the equilibrium magnetization and B_{loc} is the local magnetic field in the sample.

It follows from (13) that the decrease of B_1 with increasing distance from the coil may be compensated by Δf, which results in a spin precession around the effective field tensor. The angle Θ is obtained from

$$\operatorname{tg} \Theta = \frac{B_1}{B_0 - \omega/\gamma} = \frac{2\pi \gamma B_1}{\Delta f} \,, \tag{14}$$

where $\Delta f = (\omega_0 - \omega)/2\pi$.

Provided $\Theta = 54°44'$, $\Delta f = \sqrt{2}\pi \gamma B_1$, the application of such a sequence allows the storage of multiple NQR signals, as shown in Figure 7.

Taking (13) into account, the optimum detuning is obtained by:

$$\Delta\omega = \pm \gamma \sqrt{B_{\text{loc}}^2 + B_1^2} \,. \tag{15}$$

Then $\Delta\omega$ is dependent on the rf field B_1 level.

The results obtained indicate that spectra of samples located not too far from the coil can be detected within seconds by the NQR technique. The results support our suggestion that the NQR method might promote the solution of some analytical problems.

[1] V. S. Grechishkin, V. P. Anferov, and N. Ja. Sinyavsky, Adv. in NQR **5,** 1 (1983).

[2] V. S. Grechishkin and N. Ja. Sinyavsky, Izv. AN USSR, Fizika **42,** 2176 (1978).

[3] S. V. Anferova, V. S. Grechishkin, and N. Ja. Sinyavsky, Izv. Vusov. Fizika **I,** 110 (1985).

[4] V. P. Anferov and O. V. Starovoitova, Fizika Tvjordogo Tela (in press).

[5] V. P. Anferov and O. V. Starovoitova, J. Chimicheskoj Fiziki (in press).

[6] V. P. Anferov, V. S. Grechishkin, and N. Ja. Sinyavsky, Izv. AN USSR, Fizika **45,** 551 (1981).

[7] V. S. Grechishkin, Fiz. Tvjordogo Tela **27,** II, 3425 (1985).

[8] C. Slichter, Theory of Magnetic Resonance (Mir, M.) **1981,** p. 307.

[9] S. R. Hartmann and E. L. Hahn, Phys. Rev. **128,** 2042 (1962).

[10] J. M. Millar, A. M. Thayer, A. Bielecki, D. B. Zax, and A. Pines, J. Chem. Phys. **83,** 934 (1985).

[11] F. Noack, Progress in NQR Spectroscopy **18,** 171 (1986).

[12] D. B. Zax, A. Bielecki, K. W. Zilm, A. Pines, and D. P. Weitckamp, J. Chem. Phys. **83,** 4877 (1985).

[13] A. Bielecki, D. B. Zax, K. W. Zilm, and A. Pines, Rev. Sci. Instrum. **57,** 393 (1986).

[14] R. Kreis, D. Suter, and R. R. Ernst, Chem. Phys. Lett. **118,** 120 (1985).

[15] A. M. Thayer, J. M. Millar, and A. Pines, Chem. Phys. Lett. **129,** 55 (1986).

[16] V. S. Grechishkin and E. M. Shishkin, Izvestia Vuzov. Fizika **82,** 82 (1973).

[17] C. Amano and H. Katakura, Rev. Sci. Instrum. **56,** 103 (1985).